

THE STRUCTURE AND EMISSION SPECTRUM OF A NONRADIATIVE SHOCK WAVE IN THE CYGNUS LOOP

J. C. RAYMOND¹ AND W. P. BLAIR¹
 Harvard-Smithsonian Center for Astrophysics

AND

R. A. FESEN^{1,2} AND T. R. GULL¹
 Laboratory for Astronomy and Solar Physics, Goddard Space Flight Center
 Received 1983 March 10; accepted 1983 May 13

ABSTRACT

The ultraviolet spectrum of a Balmer-line filament located just outside the main body of optical filaments in the Cygnus Loop confirms the nonradiative shock wave theory for its origin. We extend this theory to include the hydrogen two-photon continuum, and we consider the possibility of slow electron-ion equilibration in the postshock gas. The shock velocity is inferred from the H α profile. Comparison of model calculations with optical and ultraviolet spectra favors Coulomb equilibration behind a 170 km s⁻¹ shock over models with rapid equilibration due to plasma turbulence. We find elemental abundances in the preshock gas to be typical of diffuse interstellar clouds. The ram pressure behind the shock is higher than the pressures inferred for bright optical filaments. We suggest that the bright optical filaments are regions of thermally unstable cooling behind shocks faster than the shock velocities inferred from their optical and ultraviolet spectra.

Subject headings: nebulae: abundances — nebulae: supernova remnants — shock waves — ultraviolet: spectra

I. INTRODUCTION

The bulk of the visual radiation from old supernova remnants arises in shock-heated gas which has cooled to around 10⁴ K (Cox 1972; see review by McKee and Hollenbach 1980). Comparison of the optical and ultraviolet line strengths with models of steady-flow shocks yields shock velocities of 70–130 km s⁻¹ (Raymond 1979; Benvenuti, Dopita, and D'Odorico 1980; Raymond *et al.* 1980). The commonly accepted theory for the relationship between X-ray and optical emission assumes a multiphase interstellar gas. A fast, nonradiative shock in the low-density intercloud medium (the warm neutral or warm ionized medium) produces million-degree gas and drives slower radiative shocks into the clouds which it encounters (McKee and Cowie 1975; McKee and Hollenbach 1980).

The intercloud shock produces weak, but detectable optical emission in the forbidden lines of Fe XIV and Fe X (Woodgate, Kirshner, and Balon 1977; Lucke *et al.*

1980). If it encounters neutral hydrogen, it also produces faint Balmer-line emission (Chevalier and Raymond 1978; Chevalier, Kirshner, and Raymond 1980, hereafter CKR). In the Cygnus Loop, this Balmer emission is observed as high-velocity features near the center of the remnant (Kirshner and Taylor 1976) and as a series of faint filaments several arc minutes outside the bright regions of the nebula (Raymond *et al.* 1980; Fesen, Blair, and Kirshner 1982). Optical and ultraviolet observations of such nonradiative shocks provide a unique means for direct determination of shock velocities and of elemental abundances unaffected by liberation of elements bound in grains. They also make it possible to observe directly and investigate the structure of the shock front itself as opposed to cooling gas far from the shock.

We have obtained ultraviolet spectra of the brightest portion of the series of faint filaments at the eastern limb of the Cygnus Loop. Its optical spectrum shows Balmer lines and very weak forbidden-line emission (Fesen, Blair, and Kirshner 1982, Table 1: position Q). The *International Ultraviolet Explorer* (IUE) observations reveal a continuum, which we interpret as hydrogen two-photon emission, together with lines of N V, C IV, and He II. We have also obtained further high-resolution and low-resolution optical spectra of this filament. In the low-resolution spectra, we find He I,

¹Guest Observer with the *International Ultraviolet Explorer* satellite, which is jointly operated by the US National Aeronautics and Space Administration, the Science Research Council of the UK, and the European Space Agency.

²Visiting Astronomer, Kitt Peak National Observatory, which is operated by the Association of Universities for Research in Astronomy, Inc., under contract with the National Science Foundation.

He II, and [Ne v] emission lines in addition to the [O II] and [O III] emission detected earlier. The high-resolution H α profile confirms the nonradiative shock nature of the filament and provides a measure of the shock velocity.

A shock velocity of 170–210 km s⁻¹ can account for the observed intensities of this filament. These velocities are considerably slower than $v_s \approx 350$ km s⁻¹ inferred from X-ray observations, but considerably faster than the velocities inferred from optical and ultraviolet spectra of the bright filaments. However, shocks at these velocities are required to explain O VI emission which may have been detected in the *Voyager* observations (Shemansky, Sandel, and Broadfoot 1979). The spectra suggest that electron-ion equilibration in the shocked gas proceeds by way of Coulomb collisions rather than by more rapid plasma turbulence processes and that ions are heated in a shock precursor.

II. OBSERVATIONS

A faint filament visible on the Palomar Observatory Sky Survey (POSS) prints about 5' northeast of the bright eastern region of the Cygnus Loop (NGC 6992) was found by Fesen, Blair, and Kirshner (1982) to be almost pure Balmer-line emission with a very weak (6% of H α) [O III] λ 5007 feature. This filament is the brightest section of a fairly complete line of filaments which is apparent on a very deep exposure (Gull, Kirshner, and Parker 1978). We obtained a 10.5 hr short-wavelength exposure (SWP 13410) of this filament on 1981 March 5 with the *IUE* spacecraft (described in detail by Boggess *et al.* 1978) by performing a blind offset from a nearby 10th magnitude star (20^h53^m58^s.15, +31°46'53") to the position

$$\alpha(1950) = 20^{\text{h}}53^{\text{m}}58^{\text{s}}.96, \quad \delta(1950) = +31^{\circ}45'6''.$$

The long dimension of the 10" by 20" large aperture was nearly perpendicular to the filament.

The spectrum is shown in Figure 1. Particle events and resau marks were removed from the line-by-line spectra. The background was smoothed over 50 Å and subtracted from the sum of lines 26–31. The net spectrum was then smoothed over 4.4 Å. The apparent negative values near 1370 Å and 1800 Å result from incomplete removal of particle events in the background. We obtained a second exposure of the filament on 1982 November 29 (SWP 18685) when the long dimension of the large aperture was oriented nearly parallel to the filament. Although the exposure time was only 6.1 hr, twice as much emitting area lay within the aperture, so the signal level was about the same.

Lines of N v, C IV, and He II are apparent in Figure 1. A feature at 1400 Å is marginally present in both SWP spectra. We will consider it only as an upper limit. The continuum is very noisy, but definitely present. Long exposures of blank fields with the *IUE* show spurious continuum emission at about one-quarter the

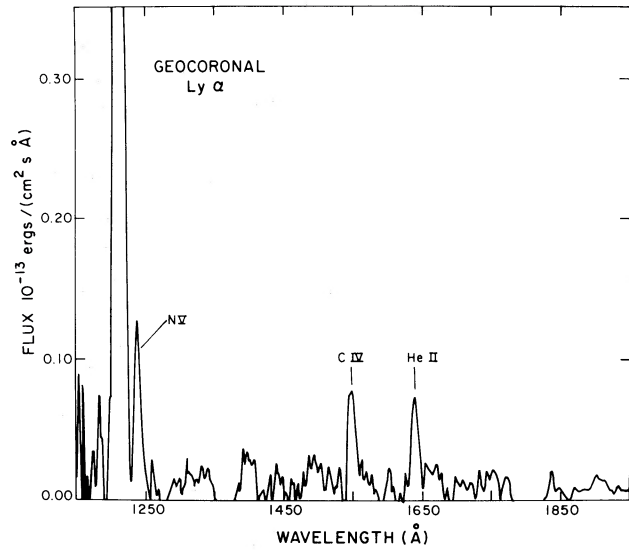


FIG. 1.—Short-wavelength *IUE* spectrum

level of these spectra, so we have reduced the apparent continuum intensities by 25% for comparison with the models. We believe the continuum to be two-photon emission from hydrogen, since no other source of continuum at these wavelengths is likely. The quality of the continuum measurement is too poor to permit verification of the two-photon spectral shape, but *IUE* observations of a bright Cygnus Loop filament have confirmed the two-photon hypothesis in that case (D'Odorico *et al.* 1980). The observed line fluxes and surface brightnesses corrected for $E(B - V) = 0.08$ (Parker 1967; Raymond *et al.* 1981) using the extinction curve of Seaton (1979) are presented in Table 1. The total continuum flux was derived from the continuum level between 1412 and 1518 Å and the theoretical spectral shape of the two-photon continuum. Based on comparison of the two spectra, we believe the line ratios to be accurate to $\pm 25\%$, while the line-to-continuum ratio is only accurate to $\pm 50\%$.

From SWP 13410, some spatial information was obtained perpendicular to the dispersion. The spectrum is appreciably wider than that obtained from a point source, but much narrower than the 20" length of the large aperture. In each of the line-by-line spectra, we have added together the 10 Å band containing the N v line. The full width at half-maximum is 4.5 pixels, compared with 2.0 pixels for a point source (de Boer and Meade 1981). Thus the width of the filament is about 5", in agreement with the apparent width of the filament on the red POSS print. This distance, about 0.019 pc assuming a distance of 770 pc, will provide a cutoff for the model integrations described below.

We have obtained further optical observations of the filament using the 2.1 m telescope and the intensified

TABLE 1
OBSERVED INTENSITIES AND DEREDDENED SURFACE BRIGHTNESSES
A. IUE OBSERVATIONS

EMISSION LINE	F_{λ} (ergs cm ⁻² s ⁻¹)		AVERAGE
	SWP 13410 ^a	SWP 18685 ^b	I_{λ} (ergs cm ⁻² sr ⁻¹)
N v λ 1240	1.2×10^{-13}	2.4×10^{-13}	2.1×10^{-4}
Si iv λ 1400	< 0.3	< 0.4	< 0.58
C iv λ 1550	0.87	1.7	1.5
He II λ 1640	0.77	1.1	1.0
C III] λ 1909	< 0.1	< 0.2	< 0.2
Two-photon	9.9	22.	16.4

B. KPNO OBSERVATIONS^c

Emission Line	F_{λ} (ergs cm ⁻² s ⁻¹)	I_{λ} (ergs cm ⁻² sr ⁻¹)
	Observed	Corrected [$E(B - V) = 0.08$]
H β	7.0×10^{-15}	1.4×10^{-5}
H δ	3.6	0.74
H γ	2.1	0.44
He I λ 3889 + H I ...	1.4	0.29
He II λ 4686	1.6	0.34
[O II] λ 3727	1.9	0.39
[O III] λ 5007	1.0	0.19
[Ne V] λ 3426	6.2	1.4

^a10'' section of filament.

^b20'' section of filament.

^c6''1 diameter aperture.

image dissector scanner (IIDS) at Kitt Peak National Observatory. Using twin 6''1 circular apertures separated by 99'' in an east-west direction, the filament was alternately placed in one aperture and then the other until a total integration time of 60 minutes was ob-

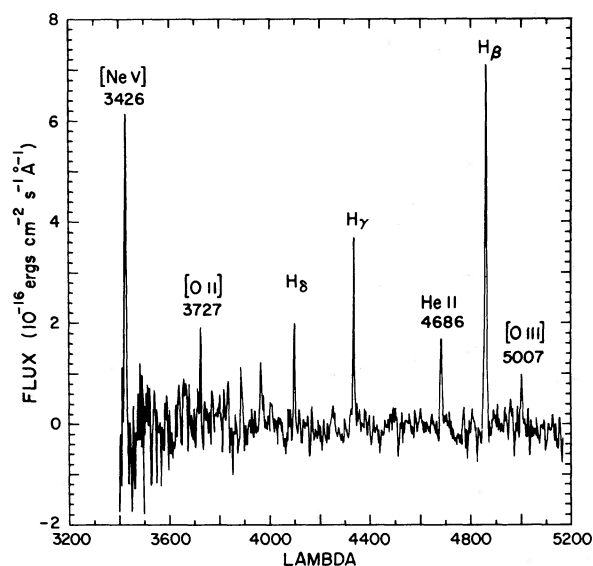
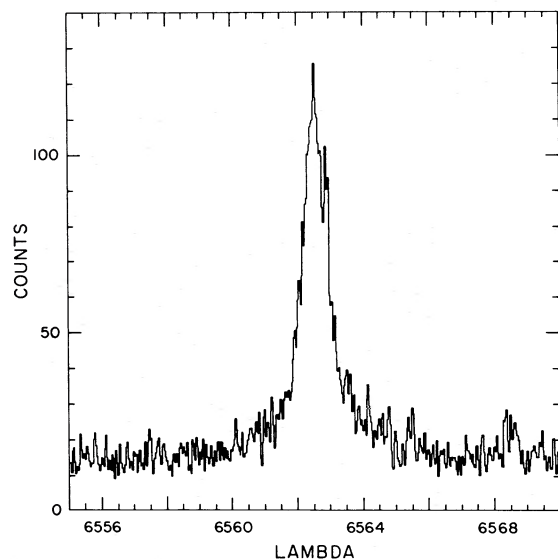


FIG. 2.—IIDS spectrum

tained. The aperture that was not on the filament at any given time was used to obtain measurements of the sky and background. The observations were calibrated using measurements of Oke (1974) white dwarf stars and the wavelength scale was established from observations of comparison lamps, using the standard reduction package at Kitt Peak. Figure 2 shows the resulting spectrum, and Table 1 lists the observed and reddening-corrected line intensities [assuming $E(B - V) = 0.08$]. By comparing the data accumulated in the east and west apertures, we estimate the relative accuracy of lines stronger than He to be $\pm 20\%$, with the exception of [Ne v], which lies very close to the end of the spectrum. Weaker lines are more uncertain. The absolute fluxes are sufficiently uncertain that we cannot combine the optical and ultraviolet fluxes for comparison with models, but the ratio of H β to the two-photon continuum is consistent with the theoretical prediction.

The [O II] intensity is also very uncertain. A large discrepancy is apparent between data from the east and west apertures of the IIDS. With the west aperture on the filament, the [O II] feature is absent to the level of the noise, while the east aperture spectrum shows [O II] intermediate in strength between H δ and H γ . If we use the low-dispersion spectrum of Fesen, Blair, and Kirshner (1982) to make an approximate calibration of the echelle spectrum discussed below, the [O II] line has

FIG. 3.—H α profile

roughly the same surface brightness as an [N II] line which we attribute to galactic background. Hence the discrepancy between the east and west aperture spectra can be understood if the [O II] line is galactic background and if it varies substantially over an arc minute. Further observations will be needed to establish whether the [O II] emission originates in the filament, and for the present we exclude this line from further consideration.

A high-resolution H α line profile was obtained at the Whipple Observatory on Mount Hopkins using the 1.5 m telescope and an echelle spectrograph with an intensified Reticon detector (Latham 1982). The projected size of the aperture was 2''.5 by 7''.5, and the long dimension was east-west. Figure 3 shows the sum of six integrations totaling 2 hours. The profile was fitted with two Gaussians. After removing the Gaussian instrumental profile (FWHM = 23 km s⁻¹), we find two components of nearly equal total intensity having full widths at half-maximum of 31 and 167 km s⁻¹. The profile is similar to that observed in the nonradiative shock on the western limb of the Cygnus Loop by Treffers (1981). The velocity centers differ by only 8 km s⁻¹, less than the uncertainty in centering the broad component. This indicates that the shock is moving almost exactly transverse to the line of sight. The least squares fitting procedure may not be appropriate if fixed pattern noise is substantial compared with photon statistics, so we have also made fits to various subsets of the data. The most important result of the fits, the width of the broad component, only varied by ± 5 km s⁻¹. Background exposures taken off the filament are too noisy to be directly subtracted from the profile, but they show that about one-fourth of the narrow component is galactic H α background, in agreement with the background

intensity found in Fabry-Perot studies of the region (R. Reynolds, private communication). Remarkably, the [N II] $\lambda 6584$ line was detected at about 5% of the total observed H α intensity. Since this intensity is consistent with Reynold's galactic background [N II]/H α ratio, and since the line is narrow, we attribute it to galactic background. Variation of both the ratio of broad to narrow components and the width of the broad component across the filament was anticipated on the basis of the models described in the next section. A search for variation of the H α width across the filament with the Multiple Mirror Telescope was unsuccessful due to the combination of a small aperture and an image intensifier with lower efficiency and higher noise level than that used on the 1.5 m telescope.

III. THEORY

The ultraviolet observations confirm the nonradiative shock theory. The intercombination lines C III] $\lambda 1909$ and O III] $\lambda 1662$ which dominate the spectra of radiative shocks (e.g., Benvenuti, Dopita, and D'Odorico 1980; Raymond *et al.* 1981) are predicted to be weak in non-radiative shocks and are not detected. The forbidden lines detected in the optical spectrum are stronger than expected, however. We now extend the theory of line emission from gas swept up by a fast shock (Chevalier and Raymond 1978; CKR; Raymond *et al.* 1980; Bychkov and Lebedev 1979) by considering lower shock velocities, two-photon emission, electron-ion equilibrium, and loss of thermal energy by excitation and ionization.

A neutral hydrogen atom swept up by a shock whose postshock temperature is very high stands some chance of being excited before it is ionized. Each neutral hydrogen atom passing through the shock front produces on average roughly four Ly α photons, 0.9 photons in the two-photon continuum, and 0.3 H α photons. The strength of any other emission line is proportional to the elemental abundance relative to hydrogen and to the excitation rate of the line divided by the ionization rate of the ion. The profiles of the Balmer lines consist of two components; a narrow component reflects the pre-shock thermal velocity distribution, while charge transfer creates a population of neutral hydrogen atoms having the bulk and thermal velocity distribution of the post-shock gas, producing the broad component.

A fast shock thermalizes three-fourths of the bulk velocity of the incoming particles, which leads to an ion temperature increase that is larger than the electron temperature increase by the ratio of masses. It is often assumed that the electron and ion temperatures are brought rapidly into equilibrium by plasma turbulence (see McKee and Hollenbach 1980), but firm evidence is lacking. The strongest observational argument for rapid equilibration is the 10–20 keV X-ray emission from Tycho's supernova remnant (Pravdo and Smith 1979). However, if the model for nonthermal X-ray emission of

SN 1006 (Reynolds and Chevalier 1981) is correct, the high-energy X-rays seen in Tycho's supernova remnant may also be nonthermal. We consider the possible effects of slower equilibration due solely to Coulomb collisions to test the rapid equilibration hypothesis with optical and ultraviolet observations.

Since the differences between the instant equilibration and slow equilibration models are fairly modest, we must choose the atomic rate coefficients with great care. We have used the distorted wave ionization rates of Younger (1981). These agree with crossed beam measurements of the ionization cross sections to within 10% for the most important ions. For several ions, inner shell excitation followed by autoionization is important. For O^+ and O^{+2} and other ions with $2p$ valence electrons, we follow the procedure of Burgess *et al.* (1977) and set the ionization potential of the $2s$ electrons equal to that of the $2p$ electrons. This gives reasonable agreement with the available measurements, but the ionization rates for these ions are less reliable than those of ions not affected by inner shell excitation. Recombination was included using rates from Aldrovandi and Pequino (1973), and the charge transfer rates used by Butler and Raymond (1980) were employed. The importance of these processes is secondary.

The excitation rates must include the temperature dependence of the collision strength. For lithium-like ions we have used the fits provided by Merts *et al.* (1980) to J. Mann's distorted wave calculations (listed in Merts *et al.*). The hydrogen excitation rates for individual angular momentum terms were taken from Aggarwal (1983), but reliable cross sections for the $n=4$ level needed to predict $H\beta$ were not available, so we multiply the predicted $H\alpha$ intensity by the Balmer decrement observed for this filament by Fesen, Blair, and Kirshner (1982). The He II $\lambda 1640$ excitation cross section was obtained from the modified Glauber calculations of Thomas (1978), and the $\lambda 4686$ rate was obtained by scaling this rate with the ratio of cross sections from Kieffer (1969). The He I $\lambda 3889$ excitation rates were taken from Kieffer's compilation of cross section measurements. The [O III] excitation cross section was taken from the distorted wave calculations of J. Mann, since these calculations extend to much higher energies than do the close coupling calculations (Baluja, Burke, and Kingston 1981). Collision strengths computed by Bhatia, Doschek, and Feldman (1979) would give [O III] intensities smaller by 30%. Collision strengths for the [O II] and [Ne v] lines were taken from Saraph, Seaton, and Shemming (1969). These collision strengths may not be accurate for the range 6–20 times the threshold energy which is most important for these models so the predicted intensities of these lines are more uncertain. Bhatia has computed [Ne v] collision strengths at energies somewhat above the range encountered in these models (listed in Merts *et al.*). Based on his computations, the

[Ne v] collision strength should be reduced by about 25%, but this is compensated by cascades from higher singlet levels.

We expect the predicted intensity of He II $\lambda 1640$ to be an underestimate. The model calculations assume that the He II Ly β line is optically thin, while the optical depth calculated from the model turns out to be near unity. Each time a He II Ly β photon is scattered, there is a 12% probability for conversion into a Ly α plus H α pair ($\lambda 304$ and $\lambda 1640$). We cannot make a reliable assessment of this effect without more accurate excitation cross sections and a radiative transfer calculation, but we expect it to roughly double the intensity of the $\lambda 1640$ line. A smaller enhancement should occur for the $\lambda 4686$ line.

Elemental abundances typical of diffuse interstellar clouds were chosen, He = 0.1, C = 1.3×10^{-4} , N = 6.2×10^{-5} , O = 4.4×10^{-4} , Ne = 8×10^{-5} , and Si = 1.1×10^{-5} (York *et al.* 1983; Ferlet 1981; Hobbs, York, and Oegerle 1982; Bruhweiler and Kondo 1982). With the exception of helium, these elements have no significant effect on the shock structure, so the models can be easily scaled to other abundances.

With these atomic rate coefficients we constructed two sets of models. The first assumes that plasma turbulence equilibrates T_e and T_i in a time short compared with any ionization or excitation time. We take preshock hydrogen densities of 1.0 and 3.0 cm^{-3} and assume the preshock gas to be 30% neutral. A higher neutral fraction would strengthen the Balmer lines compared with the forbidden lines. A larger ionized fraction would strengthen the forbidden lines relative to Balmer lines, but would weaken the two-photon continuum. The value of $30\% \pm 10\%$ is a compromise between the requirements of the ultraviolet and optical observations. Helium is assumed to be neutral. The postshock temperature is determined from the shock velocity and jump conditions. The ionization state of each element and the intensities of the important emission lines are computed for a series of short time steps. The electron and ion temperatures are kept equal, but both decline somewhat as excitation and ionization of hydrogen and helium remove some of the thermal energy of the gas. Because of this decline in temperature, a given observed width of the H α line implies a slightly higher shock velocity than would be inferred from Figure 3 of CKR, who were able to ignore the energy loss terms for the much higher shock velocity case of Tycho's supernova remnant. The observed width of 167 km s^{-1} corresponds to a shock velocity of 210 km s^{-1} . The temperature declines from about 6.5×10^5 K to 6.0×10^5 K through the region where the hydrogen lines are formed.

The second set of models assumed Coulomb equilibration alone. As indicated in Figure 3 of CKR, a given observed H α width implies a smaller shock velocity than in the equilibrium model because the kinetic

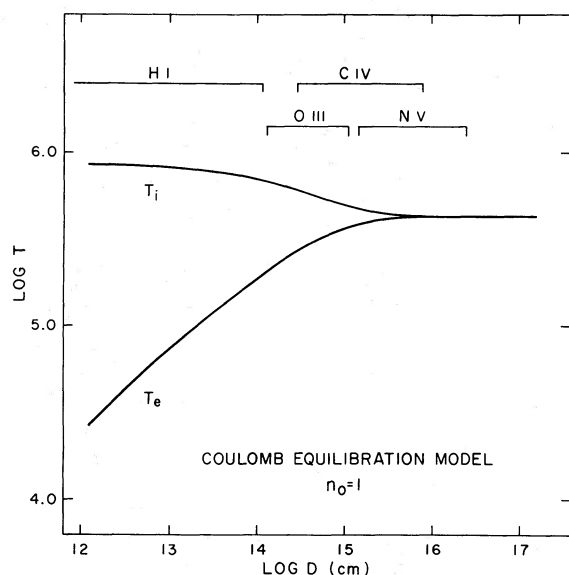


FIG. 4.—Temperature structure of Coulomb equilibration model. Ranges in which more than 10% of an element is in the observed ionization state are indicated.

energy of the ions is not divided between electrons and ions. The model is constructed by using the jump conditions for the ions alone and calculating, for a series of very short time steps, the change in T_e due to heating by Coulomb collisions with the ions (Spitzer 1978) and energy loss due to excitation and ionization. Figure 4 shows the temperature structure for an $n_0 = 1$ model and indicates the temperature ranges in which the emission lines are formed. The broad component of $H\alpha$ is formed over a broad range in ion temperature, so its profile is not a simple Gaussian. We summed the profiles calculated at each step and found that the difference between the composite profile and a Gaussian is too small to be detected in our observational data. Comparison of the observed FWHM of the broad $H\alpha$ component with the models yields a shock velocity of 170 km s^{-1} . With this shock velocity, the electrons and ions eventually equilibrate at $3.9 \times 10^5 \text{ K}$ roughly $5''$ behind the shock.

Earlier models of nonradiative shocks have assumed that the width of the narrow component is just the preshock thermal width. However, the observed 31 km s^{-1} width would give a rather high preshock temperature of $2.0 \times 10^4 \text{ K}$. Such a preshock temperature could result from heating due to photoionization by extreme-ultraviolet photons emitted by the optically bright filaments or from heating in a suprathermal particle shock precursor of the sort observed in the solar wind. However, the observed line width is sufficiently uncertain that a preshock temperature of 10^4 K cannot be excluded. In addition, the profile of the narrow component of $H\alpha$ is complicated by the radiative transfer of the

$\text{Ly}\beta$ line, so that further theoretical effort is required for any interpretation of the width of the narrow component. It is also possible that blending with the galactic background and geocoronal $H\alpha$ may make the measured width an overestimate. Thus the implications of the width of the narrow $H\alpha$ component will be deferred to a future paper. We note, however, that other measurements of narrow component widths (Treffers 1981; Kirshner and Taylor 1976) are similar to the width observed here.

It is difficult to estimate the uncertainty of the velocity determination based on the $H\alpha$ profile. The formal uncertainty of width of the best fit Gaussian is small, but we do not expect either the broad or the narrow component to be truly Gaussian. Theoretical profiles could be fitted to the data if the radiative transfer calculation for $\text{Ly}\beta$ were performed, but these would be sensitive to an additional free parameter, the preshock ion kinetic temperature. The shock velocity inferred from the line width is also weakly dependent on the neutral fraction in the preshock gas. To the extent that we are really only interested in the FWHM of the broad component, we consider $\pm 10 \text{ km s}^{-1}$ to be a reasonable estimate of the uncertainty in the shock velocity determination assuming that we can choose between Coulomb and instant equilibration models.

A further complication arises before the models can be compared with observations. In the earlier nonradiative shock models, it could be assumed that the final preshock temperature was far enough above the equilibrium temperatures of all of the observed ions that there was no contribution to the line intensities beyond a well-defined ionization zone. In the present case, the final electron temperatures are low enough that the $[\text{Ne v}]$ line (and to a lesser extent N v) is emitted from the entire postshock region. Thus we must choose a point to cutoff the integration. Based on the $5''$ apparent width of the filament ($6 \times 10^{16} \text{ cm}$ at 770 pc) and postshock velocities relative to the shock front of $v_s/4$, we terminate the integration at 360 yr for the equilibrium model and 455 yr for the Coulomb equilibration model. For a given cutoff age, the relative contribution of the region behind the initial ionization zone is proportional to the preshock density. Therefore, models having higher preshock densities differ mainly in having higher absolute surface brightnesses and relatively strong $[\text{Ne v}]$ and N v lines.

IV. DISCUSSION

The principle differences between the models result from the lower electron temperature in the Coulomb equilibration model. The lower shock velocity for a given $H\alpha$ width implies a final electron temperature 34% lower than the instant equilibration model, and for times shorter than the electron-ion equilibration time, T_e is much lower still. The greatest differences result from

TABLE 2
 PREDICTED RELATIVE INTENSITIES

EMISSION LINE	$T_e = T_i$		$T_e \neq T_i$		OBSERVED
	$n_0 = 1.0$	$n_0 = 3.0$	$n_0 = 1.0$	$n_0 = 3.0$	
N v $\lambda 1240$	1.0	1.0	1.0	1.0	1.0
Si iv $\lambda 1400$	0.04	0.04	0.03	0.03	< 0.2
C iv $\lambda 1550$	0.75	0.75	0.58	0.53	$0.64 \pm .16$
He II $\lambda 1640^a$	0.42	0.40	0.34	0.29	$0.49 \pm .12$
C III $\lambda 1909$	0.01	0.01	0.01	0.01	< 0.1
Two-photon	4.4	4.2	3.1	2.7	8.1 ± 4.0
N v photons/H	0.014	0.015	0.045	0.054	
H β (broad)	1.0	1.0	1.0	1.0	1.0 ^b
He I $\lambda 3889^c$	0.09	0.09	0.17	0.17	0.21 ± 0.07
He II $\lambda 4686^a$	0.22	0.22	0.21	0.21	0.48 ± 0.12
[O III] $\lambda 5007$	0.04	0.04	0.11	0.11	0.28 ± 0.10
[Ne v] $\lambda 3426$	0.21	0.36	0.51	1.4	1.5 ± 0.6
H β (broad) photons/H ...	0.0027	0.0027	0.0072	0.0072	

^aPredicted He II intensities underestimated; see text.

^bBroad component taken to be 0.5 observed H β intensity.

^cBlended H δ line removed by interpolation along Balmer series.

the sensitivity of the ionization rates to electron temperature. For this reason, the ions with the highest ionization potentials show enhanced line intensities in the Coulomb equilibration model, as seen by the increased number of N v photons per hydrogen atom passing through the shock and the greater strength of [Ne v]. In the relative line strengths, this is partially compensated by the increased emission of Balmer lines and two-photon continuum in the Coulomb model resulting from the relatively low electron temperature in the region where hydrogen is being ionized.

Table 2 shows that the Coulomb equilibration models fit the observations better than the instant equilibration models in that they predict stronger [Ne v] emission and somewhat stronger He I and [O III] lines. Considering the probable enhancement of He II $\lambda 1640$ by conversion of $\lambda 256$ photons, the ratio of the ultraviolet He II and N v lines also favors the Coulomb model. While the evidence is not conclusive, it is fairly strong.

The models assumed hydrogen to be 30% neutral in the preshock gas. A lower neutral fraction would decrease the intensities of the Balmer lines and the two-photon continuum relative to the other lines. Comparison of the He I and He II optical lines suggests that helium is also partially ionized in the preshock gas, since this would reduce the predicted $\lambda 3889$ intensity without affecting the $\lambda 4686$ line. The excitation cross sections for both of these lines are quite uncertain, however, so the evidence for preionization of helium is marginal.

Since liberation of elements from grains requires a longer time than the time of passage through the observed filament, we can infer the abundances in the preshock gas. The good agreement of the relative inten-

sities of the ultraviolet lines with the models indicates that the moderate depletion of the assumed diffuse cloud abundances is appropriate. This provides the initial condition for attempts to study destruction of grains in the bright optical filaments.

The models for shock emission predict the number of photons emitted in each line for each hydrogen atom flowing through the shock. These predictions can be used with an assumed preshock density and the observed surface brightness to compute the depth of the emitting filament along the line of sight. Based on the N v line, these depths are 9.8 pc or 3.0 pc for the instant equilibration, $n_0 = 1$ or 3 models, and 3.7 pc or 1.0 pc for the Coulomb equilibration, $n_0 = 1$ or 3 models. The observed length of the filament is 0.3 pc (assuming a distance of 770 pc), and this would be a reasonable guess for the depth along the line of sight. Thus the absolute line intensities favor Coulomb equilibration models and preshock densities of at least 2 cm^{-3} . Also, the Coulomb equilibration model with a preshock density as low as 1 cm^{-3} would also produce an N v filament wider than the 5'' observed. Considering the range of acceptable parameters, and the better agreement of the higher density models with the observed line ratios, we estimate the shock ram pressure, $n_0 v_s^2$, to be $8 \times 10^{14} \text{ cm}^{-1} \text{ s}^{-2}$. This is several times the pressure in the bright optical filaments of the Cygnus Loop as inferred from density-sensitive line ratios, suggesting that the filament we have observed is at an abnormally high pressure compared with the rest of the remnant. Another likely possibility is that the bright optical filaments are partially supported by magnetic pressure, so that the gas pressure measured by the optical lines

underestimates the total pressure (see Blair, Kirshner, and Chevalier 1982).

Regardless of whether the electron-ion equilibration is fast or slow, the observed shock represents a range of shock velocity not previously considered for the Cygnus Loop. X-ray observations are not sensitive to the temperatures produced by 200 km s^{-1} shocks, and the relative strengths of lines produced in the bright optical filaments are insensitive to shock velocity above 120 km s^{-1} . If steady flow were an adequate approximation, strong lines of [O I] from the recombination zone or N v from the higher temperature regions might be found associated with 200 km s^{-1} shocks, but steady flow shocks seem to be rare either because of thermal instability or clumpiness of the preshock gas (Raymond *et al.* 1981; Fesen, Blair, and Kirshner 1982). There is a strong observational bias toward filaments bright in the Balmer and [O III] lines. In thermally unstable cooling (e.g., McCray, Stein, and Kafatos 1975), this bias will tend to select regions which resemble 100 km s^{-1} shocks.

There are several theoretical consequences of the hypothesis that the bright optical filaments are produced by faster shocks than had been thought. The density contrast between cloud and intercloud gas needed to produce both the optical and X-ray emission is reduced by a factor of 2 or 3. The bright filaments would be regions of anomalously high density in the cooling flow. This would reduce the relative importance of photoionization in the optical spectra, but the magnetic pressure support suggested above would tend to increase the importance of photoionization (Raymond 1979). Thermally unstable cooling behind faster shocks would also give a larger separation between [O III]—dominated and $H\alpha$ —dominated filaments (see Fesen, Blair, and Kirshner 1982), though velocities even higher than 200 km s^{-1} might be needed to match the observed separations.

One observational consequence of the presence of 200 km s^{-1} shocks is bright O VI emission. Shemansky, Sandel, and Broadfoot (1979) reported emission at 1035 \AA from the Cygnus Loop in observations with the *Voyager* satellite. While they consider the feature to be too narrow to be the O VI doublet, there is no other plausible identification for the line. If 200 km s^{-1} shocks with preshock densities of 2 cm^{-3} represent a substantial fraction of the area of the expanding shock in the northeast part of the Cygnus Loop they could account for the brightness of the observed feature. Neither 100 km s^{-1} radiative shocks nor 400 km s^{-1} nonradiative shocks can approach the observed brightness. According to our models, the filament we have observed should be followed by a region having an O VI surface brightness of $1.2 \times 10^{-5} \text{ ergs cm}^{-1} \text{ s}^{-1} \text{ sr}^{-1}$ if the electron-ion

equilibration is slow or about 1/10 that if equilibration is rapid. The X-ray emissivity provides another test of the models. The region just inside the filament should have a $1/4 \text{ keV}$ surface brightness of $2.2 \times 10^{-4} \text{ ergs cm}^{-2} \text{ s}^{-1} \text{ sr}^{-1}$ if the rapid equilibration model holds, principally the 84 \AA line of Mg VII and the 73 \AA lines of Si VII and Si VIII. The surface brightness is $1/30$ as large according to the Coulomb equilibration model. Both these predictions assume, of course, that confusion with emission just ahead of or behind the modeled region is not a problem.

Future theoretical models will require detailed treatments of radiative transfer and shock precursors. The excitation and ionization of hydrogen remove electrons from the high-energy end of the energy distribution rapidly enough that the assumption of a Maxwellian electron distribution is questionable in the region where hydrogen is substantially neutral. The present models may underestimate the strengths of $Ly\alpha$ and the two-photon continuum relative to other emission. Future observational work should include line profile studies of other filaments and studies of the variation of the [O II] and [Ne V] lines across the filament. We also note that the Coulomb models with high preshock densities are approaching their radiative cooling times in the distance covered by the observation, so future models should include the radiative cooling terms more fully.

We note that there is substantial uncertainty in the distance to the Cygnus Loop (see Kirshner and Taylor 1976). The shock velocity determined from our observations could be used with a proper motion measurement to determine the distance accurately.

If sufficiently accurate profiles can be obtained for the extremely low surface brightness $H\alpha$ emission from the centers of supernova remnants, it will be possible to test some models for shock acceleration of cosmic rays. According to Eichler (1979), nonthermal particles can acquire as much as 50% of the energy dissipated in a shock. The broad $H\alpha$ component of a shock seen face on would show a shift equal to three-fourths of the shock velocity, but also show a width 30% lower than would be expected if all the shock energy is thermalized. Fabry-Perot observations of the Cygnus Loop (Kirshner and Taylor 1976; R. Reynolds, private communication) show that such observations are possible.

We thank R. Kirshner and the staffs of the *International Ultraviolet Explorer*, Kitt Peak National Observatory, and Whipple Observatory for aid in the acquisition of these data. This work was performed under NASA grants NAG 5-87 and NAGW-117 to the Smithsonian Astrophysical Observatory.

REFERENCES

- Aggarwal, K. M. 1983, *M. N. R. A. S.*, **202**, 15P.
 Aldrovandi, S. M. V., and Pequignot, D. 1973, *Astr. Ap.*, **25**, 137.
 Baluja, K. L., Burke, P. G., and Kingston, A. E. 1981, *J. Phys. B*, **14**, 119.
 Benvenuti, P., Dopita, M., and D'Odorico, S. 1980, *Ap. J.*, **238**, 601.
 Bhatia, A. K., Doschek, G. A., and Feldman, U. 1979, *Astr. Ap.*, **76**, 359.

- Blair, W. P., Kirshner, R. P., and Chevalier, R. A. 1982, *Ap. J.*, **254**, 50.
- Boggess, A., et al. 1978, *Nature*, **275**, 372.
- Bruhweiler, F. C., and Kondo, Y. 1982, *Ap. J.*, **259**, 232.
- Burgess, A., Summers, H. P., Cochrane, D. M., and McWhirter, R. W. P. 1977, *M.N.R.A.S.*, **179**, 275.
- Butler, S. E., and Raymond, J. C. 1980, *Ap. J.*, **240**, 680.
- Bychkov, K. V., and Lebedev, V. S. 1979, *Astr. Ap.*, **80**, 167.
- Chevalier, R. A., Kirshner, R. P., and Raymond, J. C. 1980, *Ap. J.*, **235**, 186 (CKR).
- Chevalier, R. A., and Raymond, J. C. 1978, *Ap. J. (Letters)*, **225**, L27.
- Cox, D. P. 1972, *Ap. J.*, **178**, 143.
- de Boer, K. S., and Meade, M. R. 1981, *IUE Newsletter*, No. 15, p. 53.
- D'Odorico, S., Benvenuti, P., Dennefeld, M., Dopita, M. A., and Greve, A. 1980, *Astr. Ap.*, **92**, 22.
- Eichler, D. 1979, *Ap. J.*, **229**, 419.
- Ferlet, R. 1981, *Astr. Ap.*, **98**, L1.
- Fesen, R. A., Blair, W. P., and Kirshner, R. P. 1982, *Ap. J.*, **262**, 171.
- Gull, T. R., Kirshner, R. P., and Parker, R. A. R. 1978, in *Supernovae* ed. D. Schramm (Dordrecht: Reidel).
- Hobbs, L. M., York, D. G., and Oegerle, W. 1982, *Ap. J. (Letters)*, **252**, L21.
- Kieffer, L. J. 1969, *Atomic Data*, **1**, 121.
- Kirshner, R. P., and Taylor, K. 1976, *Ap. J. (Letters)*, **208**, L83.
- Latham, D. 1982, in *IAU Colloquium 67, Instrumentation for Large Telescopes*, ed. C. Humphries (Dordrecht: Reidel), p. 259.
- Lucke, R. L., Woodgate, B. E., Gull, T. R., and Socker, D. G. 1980, *Ap. J.*, **235**, 882.
- McCray, R., Stein, R. F., and Kafatos, M. 1975, *Ap. J.*, **196**, 565.
- McKee, C. F., and Cowie, L. L. 1975, *Ap. J.*, **95**, 715.
- McKee, C. F., and Hollenbach, D. J. 1980, *Ann. Rev. Astr. Ap.*, **18**, 219.
- Merts, A. L., Mann, J. B., Robb, W. D., and Magee, N. H., Jr. 1980, Los Alamos Informal Report LA-8267-MS.
- Oke, J. B. 1974, *Ap. J. Suppl.*, **24**, 21.
- Parker, R. A. R. 1967, *Ap. J.*, **149**, 363.
- Pravdo, S. H., and Smith, B. W. 1979, *Ap. J. (Letters)*, **108**, L83.
- Raymond, J. C. 1979, *Ap. J. Suppl.*, **39**, 1.
- Raymond, J. C., Black, J. H., Dupree, A. K., Hartmann, L., and Wolff, R. S. 1981, *Ap. J.*, **246**, 100.
- Raymond, J. C., Davis, M., Gull, T. R., and Parker, R. A. R. 1980, *Ap. J. (Letters)*, **238**, L21.
- Reynolds, S. P., and Chevalier, R. A. 1981, *Ap. J.*, **245**, 912.
- Saraph, H. E., Seaton, M. J., and Shemming, J. 1969, *Phil. Trans. Roy. Soc. London, A*, **264**, 77.
- Seaton, M. J. 1979, *M.N.R.A.S.*, **187**, 73P.
- Shemansky, D. E., Sandel, B. R., and Broadfoot, A. L. 1979, *Ap. J.*, **231**, 35.
- Spitzer, L., Jr. 1978, *Physical Processes in the Interstellar Medium* (New York: Wiley).
- Thomas, B. K. 1978, *Phys. Rev. A*, **18**, 452.
- Treffers, R. R. 1981, *Ap. J.*, **250**, 213.
- Woodgate, B. E., Kirshner, R. P., and Balon, R. J. 1977, *Ap. J. (Letters)*, **218**, L129.
- York, D. B., Spitzer, L., Bohlin, R. C., Hill, J., and Jenkins, E. B. 1983, preprint.
- Younger, S. M. 1981, *J. Quant. Spectrosc. Rad. Transf.*, **26**, 329.

W. P. BLAIR and J. C. RAYMOND: Center for Astrophysics, 60 Garden Street, Cambridge, MA 02138

R. A. FESEN and T. R. GULL: Laboratory for Astronomy and Solar Physics, Code 683, Goddard Space Flight Center, Greenbelt, MD 20771